COBEM-2017-1213
EXPERIMENTAL ANALISIS OF TWO-PHASE IN A RADIAL CENTRIFUGAL PUMP

Jhoan M. C. Cubas
Henrique Stel
Edgar M. Ofuchi
Dalton Bertoldi
Moises A. Marcelino Neto
Rigoberto E. M. Morales
Multiphase Flow Research Center (NUEM), Federal University of Technology – Paraná (UTFPR). Rua Deputado Heitor Alencar Furtado, 5000. Ecoville. Curitiba – PR – Brazil.
e-mail: jhoancbs2@gmail.com; stel.henrique@gmail.com; edgarofuchi@gmail.com; daltonbertoldi@utfpr.edu.br; mneto@utfpr.edu.br; rmorales@utfpr.edu.br.

Abstract. *The presence de free gas inside centrifugal pumps cause instabilities and degradation of the pump pressure-rise curve. Depending on the intake gas fraction, liquid flow rate, intake pressure and rotational speed, this degradation can be mild or severe. Therefore, the knowledge of operating conditions and the behavior of the phases related to this performance degradation allow proper pump operation. In this scenario, this study presents an experimental work developed to perform, simultaneously, head evaluation, flow visualization and inlet gas void fraction measurement in a commercial radial pump. One of the pump impellers were reproduced in a transparent material, in order to allow flow visualization while minimizing the effect of non-original pump parts on performance. In addition, a wire-mesh sensor is used to provide actual gas void fraction measurement at the pump inlet. The images obtained were associated with the instabilities observed in the performance curves of the pump, as a way to understand the phenomena related to the performance degradation in two-phase flow operation. This procedure, together with the measurement of the actual gas volume fractions in the pump inlet, can provide an interesting source of data that can be useful to support theoretical models or validate numerical simulations.*

Keywords: *centrifugal pumps, two-phase flow, performance, visualization, wire mesh sensor.*

1. INTRODUCTION

Operation of centrifugal pumps with gas-liquid mixtures is a problem that adversely affects some processes in engineering. In pressurized water reactors, for example, two-phase flow pumping may occur and cause the so-called “loss-of-coolant accident” (LOCA). In petroleum extraction, Electric Submersible Pumps (ESP) sometimes are used in wells where gas is produced together with the oil. Pumping a gas-liquid mixture is taken as an unfavorable condition, since the presence of gas generally impairs the ability of a pump to increase pressure. Fig.1 presents a typical experimental pump head curves, one for single-phase and another for two-phase flow.

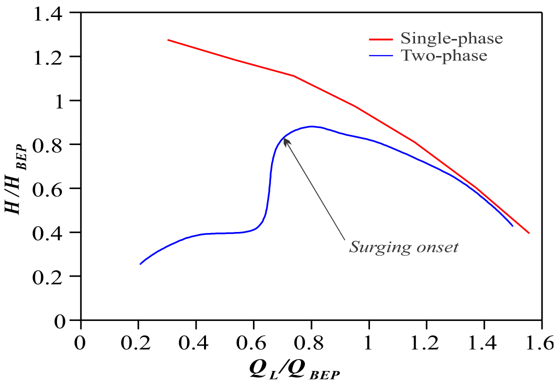

Figure 1. Typical experimental curves of pump performance under single-phase and two-phase flow.

When the liquid flow rate is reduced, it is expected that the pressure provided by the pump increases, as in single phase flow. However, what is observed is an abrupt drop in performance for two-phase flow at a certain point. This point marks the start of instabilities in the pump operation, commonly called as *surging* condition. At even lower liquid flow rates, the pump loses its ability to increase pressure almost entirely. Authors such as Estevam (2002), Barrios (2007), Gamboa (2008) associate the surging phenomenon with the presence of a gas pocket in the rotor channel.

Literature available still lacks research to better understand gas-liquid dynamics inside a pump. Mechanisms like bubble coalescence and breakup inside impellers are still poorly understood. Almost all visualization studies rely on pump modifications or prototypes, which can affect the flow dynamics and the pump performance. Another drawback of experimental works is that the void fraction of the inlet gas is mostly inferred through no-slip models, without actually measuring the gas volume fraction at the pump intake, like the one that is intended to do in this work.

2. EXPERIMENTAL PROCEDURE

Figure 2 presents an illustration (a) and a picture of the main test section (b) of the experimental arrangement developed in this investigation. It is designed to allow flow visualization, inlet gas void fraction (GVF) measurement and pressure difference evaluation of gas-liquid flows inside a centrifugal pump. A booster pump, controlled by a variable-speed drive (VSD), pulls water from a 500 liter tank, feeding the liquid line depicted in blue. The single-phase liquid properties are evaluated by a Coriolis flow meter, before being mixed with air. In turn, gas is fed into the system through an air compressor at a separated line (depicted in green). Its flow rate is controlled by a manual needle valve and is measured with an orifice-plate/capacitive-pressure-transducer system. The air is injected as dispersed bubbles into the flow loop through a gas flow mixer (porous rock). The gas-liquid mixing is done at the entrance of the flow development section, a transparent vertical pipe with a 70 mm inner diameter (D) and a length close to 20 D. This setup creates an upward bubbly flow upstream of the test pump. The centrifugal pump tested is radial-type and has two stages and a volute. Its casing and the first-stage impeller are replaced by equivalent transparent pieces to allow flow visualization, which is done by means of a high-speed camera.

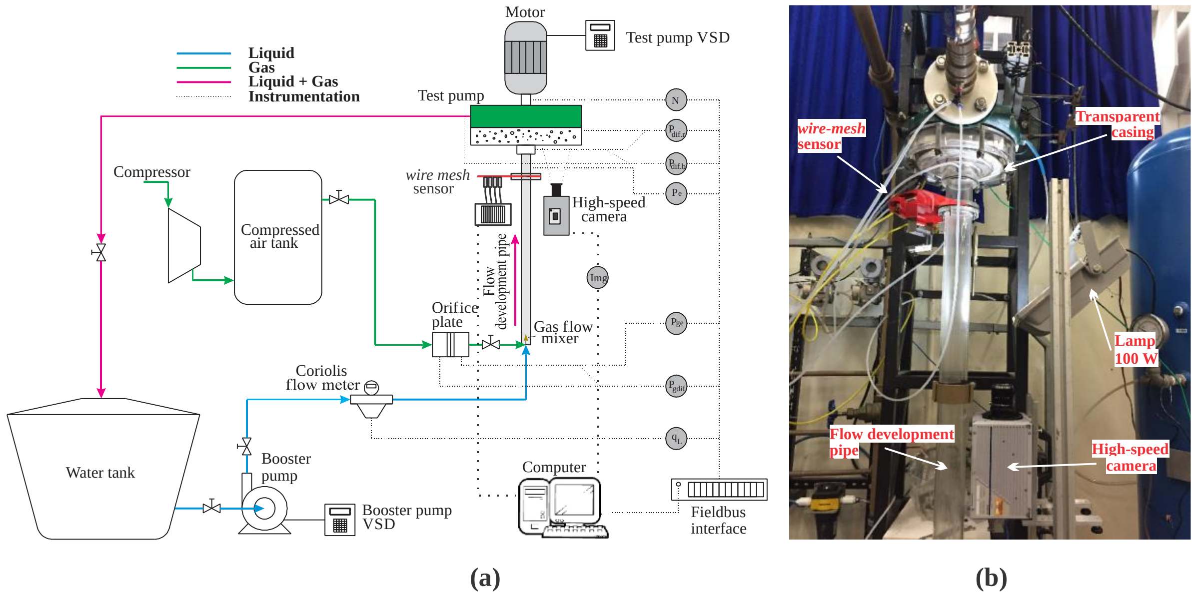

Figure 2. (a) Experimental flow loop schematic; (b) picture of main test section

A capacitive 32x32 wire-mesh sensor (Da Silva et al., 2007) is employed to evaluate the average gas void fraction (GVF) at the intake pipe cross-section. The sensor is located at, approximately, two pipe diameter (140 mm) upstream of the impeller eye, Three sets of differential pressure measurements are performed across the pump, namely, the impeller and diffuser pressure rise of the first-stage and the whole pump pressure difference. This procedure allows evaluating curves of pressure rise versus liquid flow rate at different gas volume fractions to study the effect of some operating conditions on the pump performance, which are done for a constant intake pressure (160 kPa).

3. RESULTS AND DISCUTIONS

Figure 3 presents head curves versus liquid flow rate (both normalized to their equivalent BEPs at single-phase flow) at different no-slip gas void fractions (λ) of 2, 4, 6 and 8%, according to the different rotational speeds (from 300 to 600 rpm). The no-slip gas void fraction is calculated as $\lambda = Q_g / (Q_g + Q_l)$, and$Q_g$ and Q_l are gas and liquid flow rates, respectively. In general, it is observed that the increase in the gas void fraction, always, influences the degradation of the gas-liquid performance of the pump, continuously distancing itself from the behavior obtained for the single-phase flow. However, independent of the gas void fraction value (λ), a rotational speed increase yields an increase of pump performance under two-phase flow. This improvement is better observed at 2, 4 and 6% gas void fractions where it might be noticed that the surging points have been displaced to the left or for low liquid flow rates. In practice, this displacement represents an increase of the pump operation window free of surging occurrence.

At λ=8%, operation window does not present a significant increase in a comparison with former conditions (2%, 4% and 6%), because coalescence and air pockets formation are intense at the impeller channels. This condition limits the dragging of the bubbles, decreases bubbles breaking mechanism and, lastly, inhibits liquid phase flow. A similar behavior was observed at λ=10% (not shown at Fig. 3), whereas the difference between operation windows was even less. Nevertheless, in general, an increase of gas void fraction always degrades overall pump performance.

Moreover, it can be observed that, for all the cases, in the range in which the gas-liquid pump performance presents a behavior similar to the single-phase flow (an increase of head occurs with a decrease of liquid flow rate) the rotational speed influence is imperceptible. Mainly, the pump performance curves for rotational speeds of 500 and 600 rpm, both at 2% gas void fraction, almost collapse into themselves, and even bellow surging point. This situation is justified with basis on similar phase behavior, both at impeller and diffusor, encountered for 500 and 600 rpm curves, with only a few variations in bubbles size and population.

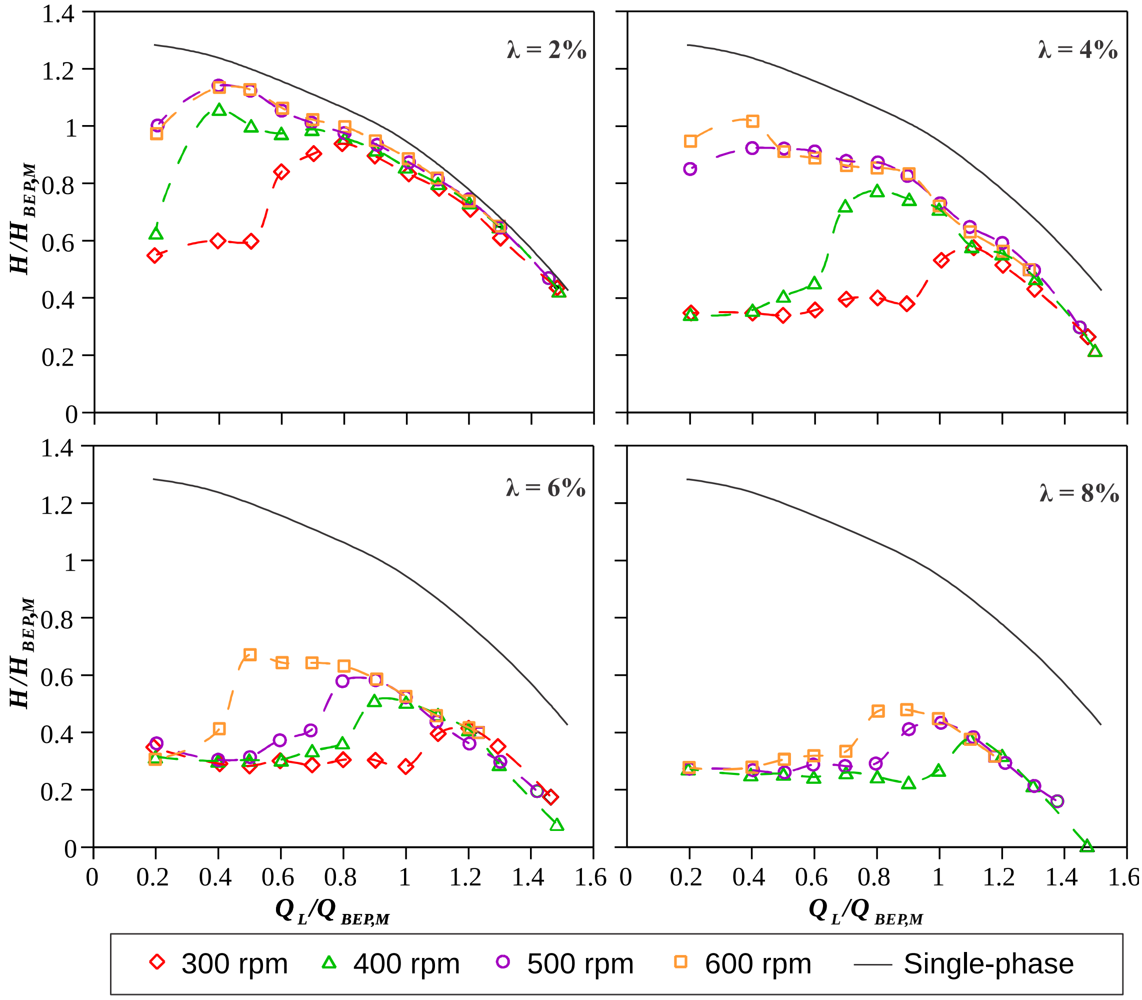

Figure 3. Normalized head as function of normalized flow rate for different no-slip gas void fraction (λ) at different rotation speeds.

Improvement of the pump performance with the increasing of the rotational speed is directly related to the effects produced over the bubbles and the phase's distribution in the impeller and diffuser channels. Some of the most important effects identified are: influence on shape and size of bubbles, influence on the transitions between phase arrangements, increase in turbulence and intensification of centrifugal field. It is supposed that turbulent effects are apparently predominant at high liquid flow rate, which causes both bubbles shearing and breaking process. In contrast, at lower liquid flow rate, centrifugal field plays a major role, generating phase separation and recirculation of liquid phase. Other interesting effect is that the turbulence and recirculation caused by impeller-diffuser interaction seem to be intensified with an increase of rotational speed, mostly at lower liquid flow rates.

Figure 4 shows the images of the phase arrangements visualized in the impeller and diffuser channels for different rotational speed (300, 400, 500 and 600 rpm), at a same gas void fraction of λ=2% and a same normalized liquid flow rate of 0.5. It can be seen that, the rotational speed increase yields, in general, a reduction of bubble diameter and a growth in the bubbles population. For 300 rpm, the bubbles have a bigger size and irregular shape with a small bubbles population. While, for 500 rpm the bubbles shape tends to be more regular and smaller in size. This behavior was observed at both the impeller and diffuser channels. Furthermore, the rotational speed increase also influences the behavior between the phase arrangements. Although the three tests evaluated (300, 400 and 500 rpm) are performed under the same operating conditions, the visualization analysis reveals different phase arrangements in each rotational speed. At 300 rpm, there is a gas pocket in all impeller channels; at 400 rpm, there is a bubble agglomeration (moderate coalescence); for 500 rpm, there is a bubble flow, with agglomeration, but without coalescence.

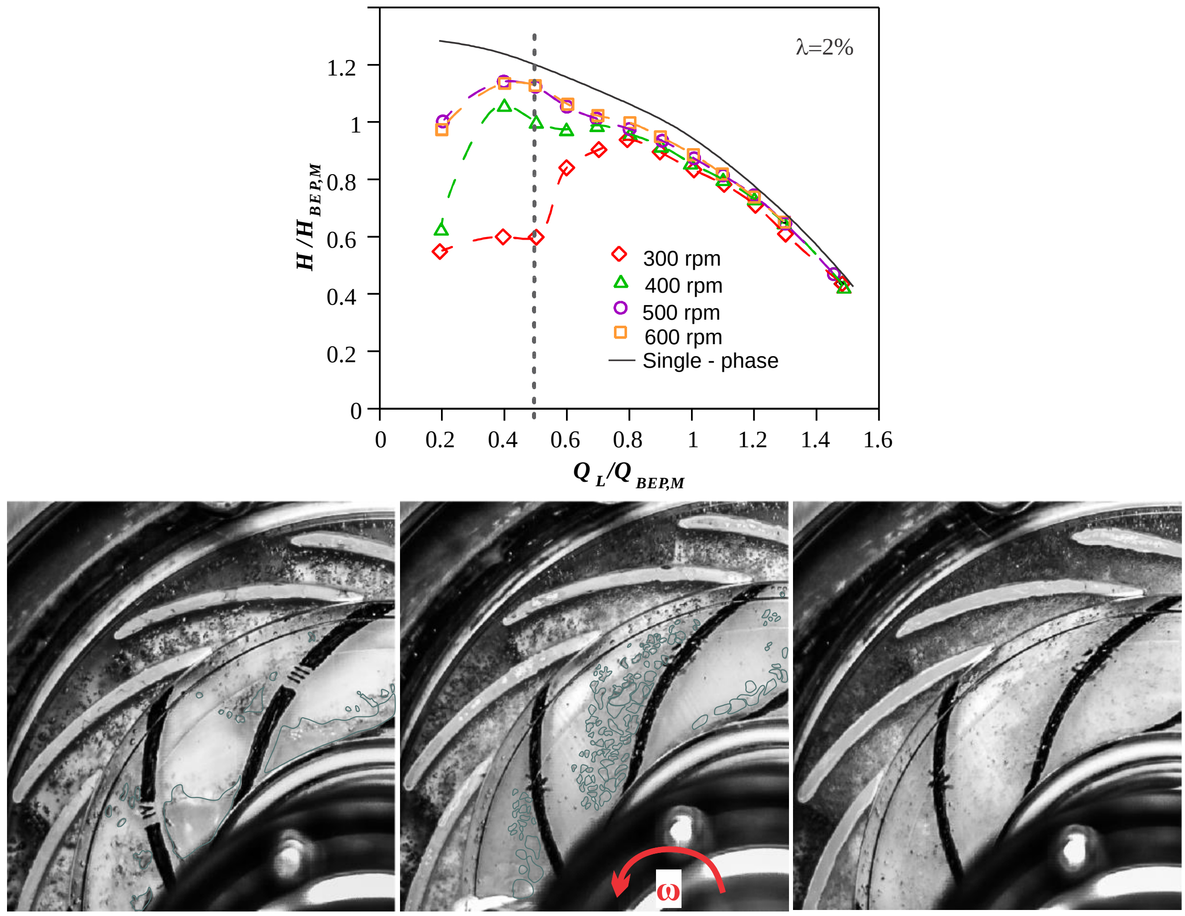

λ=2% - 300 rpm λ=2% - 400 rpm λ=2% - 500 rpm

Figure 4. Images of flow patterns at $Q_l/Q_{BEP,M}$ = 0.5, λ = 2% and different rotational speed.

In general, each phase arrangements (flow pattern) is associated with a certain performance degradation. In general, with higher gas accumulation and permanence in the impeller channels, the performance degradation will be greater. Then, as seen in the visualization images for the three rotational speeds, as the rotational speed increase there is a less gas accumulation in the impeller channels, which will increase the pump performance. These difference in flow patterns between the rotational speeds can be attributed, as one of the main factors, to the magnitude with which the effects resulting from the centrifugal field and the liquid phase pressures act, which, for the operating conditions shown in the figure correspond to a condition of part-load. In this operating condition, Gülich (2010) indicated that liquid phase recirculations are a consequence of the centrifugal field, and that they can promote phase’s mixing and thus improve the gas handling pump capacity. Therefore, as is known, increasing the rotational speed intensifies the centrifugal field at the pump, thereby intensifies the recirculation and turbulence of the liquid phase, which in turn generate a continuous bubbles breaking, decreasing their size. As a rule, the decrease in bubbles size is favorable so that they can get out of the impeller channels with less difficulty. This effect is shown in the work of Jiménez (2016), where the author verified that the smaller bubbles could leave the impeller more easily than the larger bubbles, thus avoiding the bubbles recirculations and consequently the gas pocket formation.

Visualization images, also, confirmed that the intensity of the recirculations throughout the impeller channels became larger with the rotational speed increase, which caused an intense bubble break and avoided the gas pocket formation. This can be seen for 500 rpm in which the bubble size and population in the impeller and diffuser channels decrease compared to the rotational speed of 300 and 400 rpm, in which there is gas pocket formation and strong agglomeration with coalescence, respectively.

On the other hand, it was also observed, and confirmed, that the surging phenomenon onset occurred when there was gas pocket formation in all impeller channels. It was also seen that the shape and behavior of these gas pockets change with the increase in rotational speed as shown in Fig. 5, which presents the images of the gas pockets in the surging onset condition for at the same no-slip gas void fraction, λ=6% and with rotational speed of 300, 400, 500 and 600 rpm.

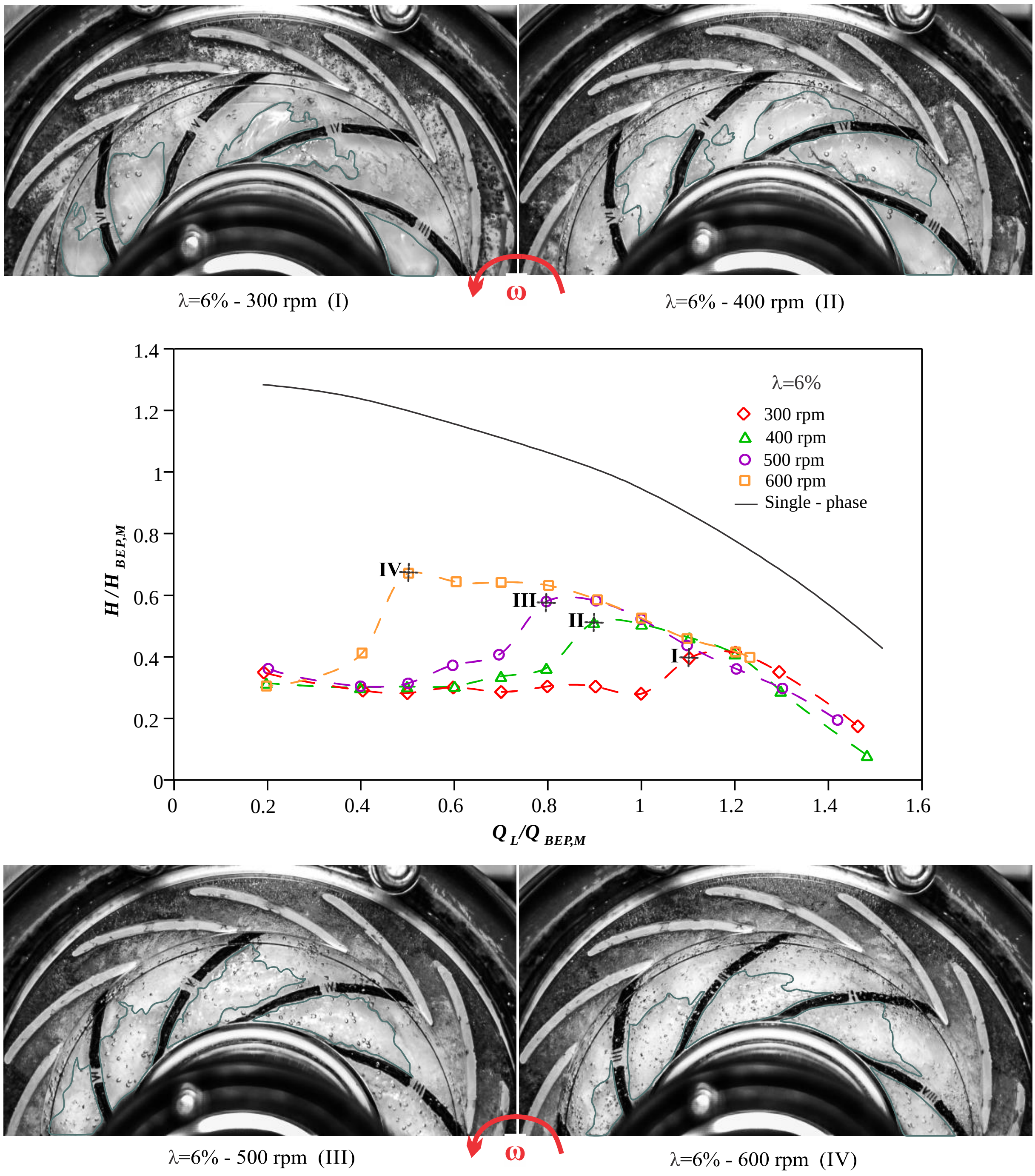

Figure 5. Images of the gas pocket shape at the points of surging onset for a no-slip gas void fraction of λ=6% and different rotational speed.

At 300 e 400 rpm, the gas pockets are unstable and continuously deformed by the liquid phase passage. In some impeller channels, the liquid phase has enough energy to cross through the gas pocket, dividing it in two parts or pushing the gas pocket against one of the channels side, and then to flow through the other half of the impeller channel. This behavior can be seen in the channels contained between blades V and VI for 300 and 400 rpm. The gas pocket breaking is slight, giving rise, in few cases, to other smaller gas pockets that tend to keep recirculating and coalescing near the impeller outlet. With the rotational speed increase to 500 and 600 rpm, it is observed that the gas pockets are more stables and tend to occupy the impeller channels in a more homogeneous way, that is, the gas pockets remain practically fixed from the impeller inlet to a little more than the transverse half of channel, without suffering considerable deformations with the liquid phase passage in form of film around it. Bubble break is intense downstream of gas pocket where, in the interface between the liquid and gaseous phase, a dense dispersion of small bubbles appears.

This change in the shape of the gas pocket can be attributed to the adverse pressure gradient to the flow in the impeller channels, which grows quadratically with rotational speed increase. This causes the force due to the pressure gradient to increase and is greater at high rotational speeds. Therefore, the intensity with which this force acts on the gas pocket by pushing it and compressing it in the direction of the impeller channels inlet is greater for the rotational speed of 500 and 600 rpm than for 300 and 400 rpm. It is understood that, for this reason, the gas pocket, for high rotational speeds, are more stables and occupy the impeller channels more evenly, dividing them into two well-defined regions: (i) active region (downstream of gas pocket) and (ii) almost inactive (occupied by the gas pocket). Furthermore, it has noted that rotational speed increase causes the bubbles, product of the break downstream of gas pocket, to be able to exit the impeller channels, since the liquid phase flow rate increases proportionally with the rotational speed. This allows the liquid phase to gain a little kinetic energy in this region of the impeller (active region), that will help decrease the performance degradation. Already for lower rotational speed, the majority of these bubbles tend to stay in the impeller, subject to recirculation and coalescence.

In general, improved pump performance due a rotational speed increase can be attributed to the intensification of turbulence and of recirculations of liquid phase, which promote bubbles breaking and delay the gas pocket formation. However, depending on the operating region of the pump, the bubble breaking is caused by two different phenomena. For instance, for liquid flow rates below the best efficiency point (BEP), the liquid phase recirculations, product of the centrifugal field (Gülich, 2010), are which promote bubbles breaking and phases mixing. In turn, for high liquid flow rates, the bubbles breaking is attributed to the high liquid phase velocities that cause a high turbulence.

On the other hand, it is known that the increase of rotational speed also increases the pressure gradient quadratically, whereas the liquid flow rate increases linearly (the pumps similarity theory). Thus, the increase in pressure gradient force is greater than that of the drag force. However, the drag force is proportional to the bubble diameter squared, while the pressure gradient force is proportional to the cube diameter. This causes the net force of the pressure gradient acting on the bubbles, at 500 and 600 rpm, to be reduced. Then, as noted, the rotational speed increase promotes the breaking and reduction of bubbles size, thereby reducing the influence of the pressure gradient force on them, which allows the liquid phase to entrain the gas phase out of impeller channels with easier. It is important to indicate that the behavior and magnitude of each of these parameters may be sensitive to the pump operating point or region.

Figure 6 presents the gas void fraction measurements with wire-mesh sensor, at pump inlet, and those calculated by drift-flux model (Zuber and Findlay, 1965) for upward dispersed bubbly flow (for a constant and no-slip gas void fraction of λ=4%) according to different operational conditions.

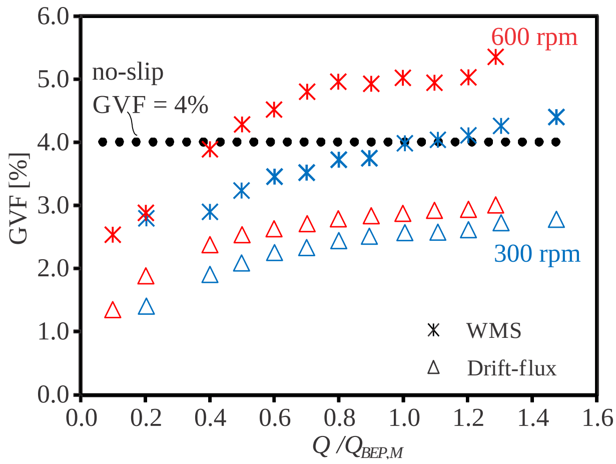

Figure 6. Gas void fraction obtain assuming the drift-flux model and those measurements with wire mesh sensor, for no-slip gas void fraction λ=4% at different operating conditions.

It can be observed that void fractions obtained with wire-mesh sensor present better agreement with those calculated with homogeneous model (non-slip) than that calculated by drift-flux model. For liquid flow rates over those ones, where homogenous model and wire-mesh present the same results, homogenous model underestimates void fraction in comparison to wire-mesh sensor data. On the other hand, for liquid flow rates below those ones, where homogenous model and wire-mesh present the same results, homogenous model overestimates void fraction in comparison to wire mesh sensor data. Void fraction is underestimated by drift-flux model independent of the scenario. It can be noticed, as well, that void fraction obtained from wire-mesh is sensitive to rotational pump speeds. The difference between wire-mesh and homogeneous model (non-slip) results indicate a limitation of using a homogenous model to estimate void fraction or gas flow rate in order to determinate a two-phase flow performance curve.

4. CONCLUSIONS

This work aims to contribute on understanding the complex phenomenon of gas-liquid flows in centrifugal pumps. Performance evaluation, gas void fraction (GVF) measurement and high-speed photography were all put together to comprehend how the gas-liquid flow pattern inside a pump affects its performance at different operating conditions. Results showed that performance deterioration is mostly associated to the gas-phase coalescence inside the pump channels, causing the liquid phase to flow in a condition that is far from the pump design. However, increasing the impeller speed generally hinders bubble coalescence, and their diameter diminishes on average, attenuating the head degradation. The actual GFV measured at the pump intake remains close to the estimated no-slip GVF for most part of the pump operational window, but a great departure from both is seen for operation at part-load liquid flow rates. This information could be useful to guide analytical correlations for head estimation in pumps operating with gas-liquid flows, as well as to provide valuable inputs for numerical simulations.

5. ACKNOWLEDGEMENTS

The authors are thankful to the TE/CENPES/PETROBRAS for the financial and technical support for this study.

6. REFERENCES

Barrios, L. J., 2007. *Visualization and Modeling of Multiphase Performance inside an Electrical Submersible Pump*. PhD thesis, The University of Tulsa, Oklahoma, USA.

Da Silva, M. J., Schleicher, E., and Humpel, U., 2007.“Capacitance wire-mesh sensor for fast measurement of phase fraction distributions”. *Measurement Science and Technology*, Vol. 18, p. 2245-2251.

Estevam, V., 2002. *A phenomenological analysis about centrifugal pump in two-phase flow operation*. PhD thesis, Unicamp, Campinas, Brasil.

Gamboa, J., 2008. *Prediction of the Transition in Two-Phase Performance of an Electrical Submersible Pump*. PhD thesis, The University of Tulsa, Oklahoma, USA.

Gülich, J. F., 2010. *Centrifugal Pumps*. Springer, Berlin, 2nd edition.

Jiménez, F. C. A., 2016. *Numerical Analysis of the Dynamics of an Isolated Gas Bubble on a Centrifugal Pump Impeller*. Msc Dissertation, Universidade Tecnologica Federal do Paraná, Curitiba, Brazil.

Zuber, N. and Findlay, J. A., 1965.“Average Volumetric concentration in two-phase flow System”. *Journal of Heat Transfer*, Vol. 87, p. 453 – 468.

7. RESPONSIBILITY NOTICE